Crossed Molecular Beam Studies of the Reactions of Allyl Radicals, $C_3H_5(X^2A_2)$, with Methylacetylene ($CH_3CCH(X^1A_1)$), Allene ($H_2CCCH_2(X^1A_1)$), and Their Isotopomers

Y. Guo,[†] A. M. Mebel,[‡] F. Zhang,[†] X. Gu,[†] and R. I. Kaiser*,[†]

Department of Chemistry, University of Hawaii at Manoa, Honolulu, Hawaii 96822, and Department of Chemistry and Biochemistry, Florida International University, Miami, Florida 33199

The chemical dynamics of the reaction of allyl radicals, $C_3H_5(X^2A_2)$, with two C_3H_4 isomers, methylacetylene ($CH_3CCH(X^1A_1)$) and allene ($H_2CCCH_2(X^1A_1)$) together with their (partially) deuterated counterparts, were unraveled under single-collision conditions at collision energies of about 125 kJ mol^{-1} utilizing a crossed molecular beam setup. The experiments indicate that the reactions are indirect via complex formation and proceed via an addition of the allyl radical with its terminal carbon atom to the terminal carbon atom of the allene and of methylacetylene (α-carbon atom) to form the intermediates $H_2CCHCH_2CH_2CCH_2$ and $H_2CCHCH_2CHCCH_3$, respectively. The lifetimes of these intermediates are similar to their rotational periods but too short for a complete energy randomization to occur. Experiments with D4-allene and D4-methylacetylene verify explicitly that the allyl group stays intact: no hydrogen emission was observed but only the release of deuterium atoms from the perdeuterated reactants. Further isotopic substitution experiments with D3-methylacetylene combined with the nonstatistical nature of the reaction suggest that the intermediates decompose via hydrogen atom elimination to 1,3,5-hexatriene, $H_2CCHCH_2CHCCH_2$, and 1-hexen-4-yne, $H_2CCHCH_2CCCH_3$, respectively, via tight exit transition states located about 10−15 kJ mol^{-1} above the separated products. The overall reactions were found to be endoergic by 98 ± 4 kJ mol^{-1} and have characteristic threshold energies to reaction between 105 and 110 kJ mol^{-1}. Implications of these findings to combustion and interstellar chemistry are discussed.

1. Introduction

During the last decades, the reaction dynamics of resonantly stabilized free radicals (RSFRs) such as the allyl radical, C_3H_5 (X^2A_2), have attracted considerable attention both from the experimental and theoretical viewpoint.[1] Here, RSFRs are considered as important growth species in the formation of polycyclic aromatic hydrocarbons (PAHs) and soot[2] during the combustion of hydrocarbon-based fuels.[3] The role of allyl radicals in the chemical vapor deposition (CVD) yielding diamonds has been pointed out recently.[4] Due to the delocalization of the unpaired electron, resonantly stabilized free hydrocarbon radicals are more stable than ordinary radicals.[5−13] Therefore, RSFRs are relatively unreactive and can reach high concentration in flames. These high concentrations make them important in the mechanism of formation of complex hydrocarbons such as the very first aromatic ring species in combustion systems.[14]

Due to the importance of allyl radicals in combustion flames and CVD processes, the underlying kinetics of allyl radical reactions with unsaturated hydrocarbons have been investigated in depth during the last decades.[15] These studies suggested relatively low rate constant in the order of 10^{-12} to 10^{-14} cm^3 s^{-1} under combustion chemistry conditions with temperatures of up to 2500 K.[16] Those low rate constants could be indicative of entrance barriers (activation energies) and/or of strongly endoergic reactions. However, despite ample kinetic studies, information on the reaction products and the inherent dynamics are sparse. The crossed molecular beam experiments of allyl

radicals with ground-state oxygen atoms, $O(^3P_j)$,[17] presents the only dynamics studies published so far. Considering the absence of dynamics information of allyl radical reactions with unsaturated hydrocarbon molecules, we investigated in the present study the chemical dynamics of the reactions of ground-state allyl radicals, $C_3H_5(X^2A_2)$, with two C_3H_4 isomers, methylacetylene ($CH_3CCH(X^1A_1)$) and allene ($H_2CCCH_2(X^1A_1)$), under single-collision conditions as provided in crossed molecular beam experiments.

2. Experiments and Methods

2.1. Experimental Setup. The scattering experiments were conducted under single-collision conditions in a crossed molecular beam machine at The University of Hawaii.[18] Briefly, a pulsed supersonic beam of allyl radicals was generated via flash pyrolysis of allyl iodide (C_3H_5I; TCI) in the primary source chamber employing a modified Chen source[19] coupled to a piezoelectric pulsed valve.[20] Here, 3040 torr of helium gas (Mattheson, 99.9999%) was introduced into a stainless steel reservoir, which contains the allyl iodide sample. This unit was kept at 253 K so that the concentration of allyl iodide is less than 0.1%. This mixture was expanded at a stagnation pressure of 780 torr through a resistively heated silicon carbide tube; the temperature of the tube was estimated to be around 1200−1500 K. The pulsed valve was operated at 200 Hz with pulses between 80 and 150 μs wide. Under these conditions, the decomposition of the allyl iodide precursor to the allyl radical and atomic iodine is *quantitative*. After passing a skimmer, a four-slot chopper wheel selected a component of the allyl radical beam with a peak velocity v_p of about 3400 ms^{-1} (Table 1).

　　　[†] University of Hawaii at Manoa.
　　　[‡] Florida International University.

Reactions Dynamics of $C_3H_5(X^2A_1)$ with C_3H_4 Isomers

J. Phys. Chem. A, Vol. 111, No. 23, 2007 **4915**

TABLE 1: Peak Velocities (v_p), Speed Ratios (S), Center-of-Mass Angles (Θ_{CM}), Together with the Nominal Collision Energies (E_c) of the Reactants

beam	v_p (ms^{-1})	S	E_c (kJ mol^{-1})	$\Theta_{CM}{}^a$
$CH_3CCH(X^1A_1)$	870 ± 12	12.5 ± 1.0		
$CD_3CCD(X^1A_1)$	860 ± 15	12.5 ± 1.0		
$CD_3CCH(X^1A_1)$	863 ± 15	12.5 ± 1.0		
$C_3H_5(X^2A_2)$/He	3403 ± 46	8.2 ± 0.6	124.9 ± 3.4	14.0 ± 0.4
$H_2CCCH_2(X^1A_1)$	894 ± 12	12.5 ± 1.0		
$D_2CCCD_2(X^1A_1)$	880 ± 15	12.5 ± 1.0		
$C_3H_5(X^2A_2)$/He	3392 ± 52	7.4 ± 0.7	124.6 ± 3.8	14.4 ± 0.4

^{a} CM angle with respect to the nondeuterated reactants. The speed ratio is defined via eq 1 with $\alpha = [(2RT)/m]^{-1/2}$ with m being the mass of the species, R the ideal gas constant, and T the temperature of the beam.

We estimated a number density of about 10^{13} allyl radicals cm^{-3} in the interaction region; this is a similar order of magnitude compared to the supersonic carbon atom beams.[21] This allyl radical beam crossed at a right angle with a neat and pulsed methylacetylene, $CH_3CCH(X^1A_1)$ (Linde; 99.8%), or allene, $H_2CCCH_2(X^1A_1)$ (Aldrich; 99.5%), released by a second pulsed valve at a pressure of 550 torr under well-defined collision energies (Table 1). To elucidate on the position of the hydrogen atom loss, we also conducted experiments with D4-allene (D_2CCCD_2; CDN; 99% + D), D4-methylacetylene (CD_3CCD; CDN; 99% + D), D3-methylacetylene (CD_3CCH; CDN; 99% + D), and D1-methylacetylene (CH_3CCD; CDN; 99% + D).

It is important to comment briefly on the bath temperature of the allyl iodide sample. First, we tried to keep the temperature at 233 K. At these conditions, the decomposition of the precursor is quantitative; elastic scattering experiments with neon clearly indicate that only allyl radicals and iodine atoms are produced. However, when crossing this beam with allene/methylacetylene, only a very weak signal was observed even at the center-of-mass angle. This made the reactive scattering experiments not feasible. Therefore, we decided to increase the bath temperature stepwise up to 253 K; higher bath temperatures should be avoided to prevent recondensation of allyl iodide inside the pulsed valve. At 253 K, the allyl radical beam is stronger by a factor of up to 4. On the other hand, an on-axis analysis and scattering experiments with neon depicted the existence of small amounts (<0.5% with respect to allyl) of C_6H_{10}, i.e., the radical−radical recombination product of the ally radical self-reaction, detected via its mass-to-charge ratio, m/z, of 82. However, the relatively intense allyl radical beam at 253 K made the crossed beam reactions with allene and methylacetylene feasible and reduced the experimental times to only 1 month per system. The effect of C_6H_{10} on the scattering signal is discussed in the Results together with the recorded time-of-flight (TOF) data and laboratory frame (LAB) distributions.

The scattered species were monitored using a quadrupole mass spectrometric detector in the TOF mode after electron impact ionization of the molecules. The detector could be rotated within the plane defined by the primary and the secondary reactant beams to take angular resolved TOF spectra in steps of 1.5°/2.0°. By integrating the TOF spectra at distinct laboratory angles, we obtained the laboratory angular distribution, i.e., the integrated signal intensity of an ion of distinct m/z versus the laboratory angle. Finally, information on the chemical dynamics was extracted by fitting these TOF spectra and the angular distribution in the LAB using a forward-convolution routine.[22] This approach initially assumed an angular distribution $T(\theta)$ and a translational energy distribution $P(E_T)$ in the center-of-mass reference frame (CM). Since the previous kinetic studies of allyl

radical reactions with unsaturated hydrocarbons showed the existence of threshold energies to reaction, E_o,[23] we incorporated an energy-dependent cross section, $\sigma(E_c) \sim [1 - E_o/E_C]$, via the line-of-center model with the collision energy E_C for $E_C \geq E_o$ in the fitting routine.[24] Note that there are currently no reliable data on the collision energy dependence of the cross section; in these cases, the line-of-center model is often utilized as a simplified model. TOF spectra and the laboratory angular distribution were then calculated from these center-of-mass functions. Due to the low signal counts, we had to accumulate up to 8×10^6 TOF spectra to obtain a reasonable signal-to-noise ratio of the reactively scattered species. This limited us to conduct the experiments with the (partially) deuterated reactants only by recording TOF spectra at the center-of-mass angles. The final outcome is the generation of a product flux contour map. This presents the differential cross section, $I(\theta, u) \sim P(u) \times T(\theta)$, of the product which reports the intensity of the heavy reaction product as a function of angle θ and product center-of-mass velocity u. This map serves as an image of the reaction and contains all the information of the reactive scattering process.

$$N(v) = v^2 \exp\left[-\left(\frac{v}{\alpha} - S\right)^2\right] \tag{1}$$

2.2. Electronic Structure and Statistical Calculations. The geometries of reactants, products, various intermediates, and transition states on the C_6H_9 potential energy surfaces for the reactions of allyl radical with methylacetylene and allene were optimized using the hybrid density functional B3LYP method with the 6-311G(d,p) basis set.[25,26] Vibrational frequencies were computed at the same theoretical level in order to characterize stationary points as local minima and transition states (the number of imaginary frequencies equals to 0 and 1, respectively), to obtain zero-point energy (ZPE) corrections, and to be used in RRKM calculations of reaction rate constants and relative product yields. The energies were then refined by single-point calculations using the G3(MP2,CCSD)//B3LYP method,[27] which approximates the coupled cluster[28] CCSD(T)/G3MP2 energy. All calculations were carried out using the GAUSSIAN 98[29] and MOLPRO 2000[30] programs. The average absolute deviation of the G3(MP2,CCSD)//B3LYP method for enthalpies of formation of 148 molecules from the G3 test set is 5 kJ mol^{-1}. Note that we used RRKM theory for computations of rate constants of individual reaction steps.[31] Rate constant $k(E)$ at an internal energy, E, for a unimolecular reaction $A^* \rightarrow A^{\ddagger} \rightarrow P$ can be expressed via eq 2, where σ is the reaction path degeneracy, h is Plank's constant, $W^{\ddagger}(E - E^{\ddagger})$ denotes the total number of states for the transition state (activated complex) $A^{\ddagger}$ with a barrier $E^{\ddagger}$, $\rho(E)$ represents the density of states of the energized reactant molecule A^*, and P is the product or products. The calculations were performed at different values of the internal energy E computed as a sum of the energy of chemical activation (the relative energy of an intermediate or a transition state with respect to the initial reactants) and the collision energy E_c. The rate constants calculated for individual reaction steps were then used to compute relative yields of different products.

$$k(E) = \frac{\sigma}{h} \frac{W^{\ddagger}(E - E^{\ddagger})}{\rho(E)} \tag{2}$$

3. Results

3.1. Laboratory Data. In our crossed beam experiments of allyl radicals with methylacetylene and allene, we recorded reactive scattering signal at mass-to-charge ratios, m/z, from m/z
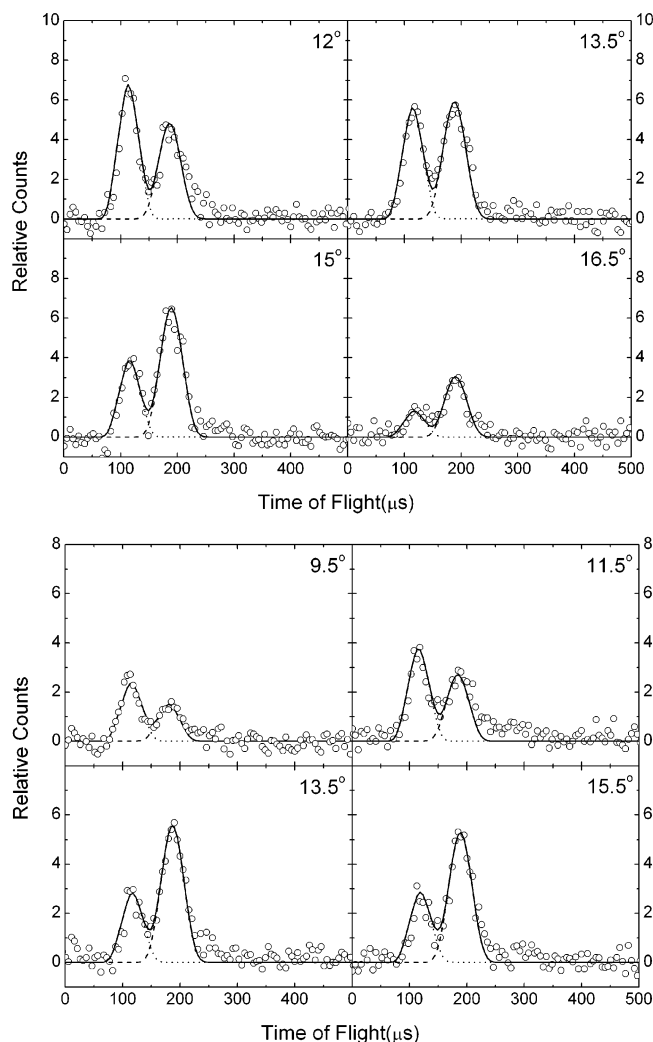
Figure 1. Selected time-of-flight data for $m/z = 80$ ($C_6H_8^+$) recorded at collision energies of 124.9 (allyl−methylacetylene; top) and 124.6 kJ mol^{-1} (allyl−allene; bottom) at various laboratory angles. The circles indicate the experimental data, the dashed, dotted, and solid lines the calculated fits for the reactive channel, the elastic channel, and the sum.
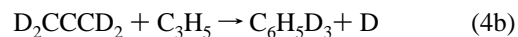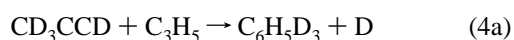
$= 80$ ($C_6H_8^+$) to 78 ($C_6H_6^+$) for both systems (Figure 1). Within this mass range, the TOF spectra are—after scaling— superimposable. Note that the TOF spectra consist actually of two distinct peaks. If we investigate higher masses, we can also observe signal at $m/z = 82$ ($C_6H_{10}^+$) and 81 ($C_6H_9^+$); however, for these masses, the slow component vanishes; only the fast peak remains virtually unchanged. Also, when conducting a scattering experiment of the primary beam with neon, the fast peak stays and the slow peak disappears. These findings suggest that the fast component originates from scattered C_6H_{10} molecules, i.e., the product of the allyl radical−allyl radical recombination detected via its mass-to-charge ratios from $m/z = 82-78$. The slow component, which is only detectable at m/z ratios of 80 and lower, comes from reactive scattering of the allyl radical with allene/methylacetylene. Summarized, the interpretation of the TOF data suggests that only the atomic hydrogen replacement channel is open within this mass regime to form molecule(s) with the generic formula C_6H_8 (eq 3); the molecular hydrogen replacement channels are closed.

$$CH_3CCH + C_3H_5 \rightarrow C_6H_8 + H \quad (3a)$$

$$H_2CCCH_2 + C_3H_5 \rightarrow C_6H_8 + H \quad (3b)$$
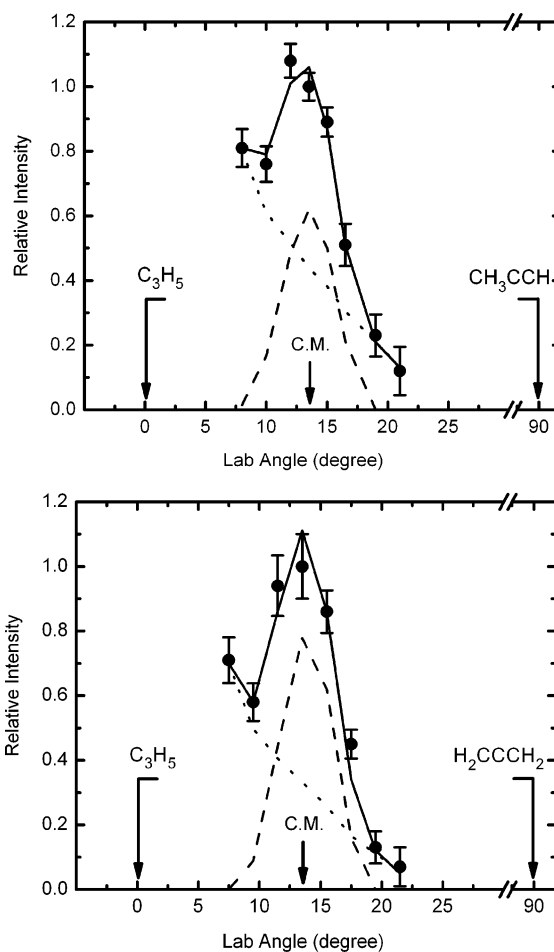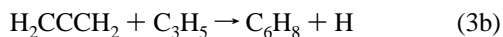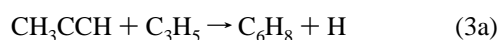
Figure 2. Corresponding laboratory angular distribution of the C_6H_8 product recorded at $m/z = 80$ for the reactions of the allyl radical with methylacetylene (top) and allene (bottom). The circles indicate the experimental data, the dashed, dotted, and solid lines the calculated fits for the reactive channel, the elastic channel, and the sum.

TOF data obtained at lower masses such as from $m/z = 66$ ($C_5H_6^+$) to $m/z = 64$ ($C_5H_4^+$) show the same patterns as those TOF recorded at $m/z = 80-78$; therefore, we can conclude that the methyl group elimination pathway is not open under our experimental conditions. The corresponding laboratory angular distributions are shown in Figure 2. Clearly, two channels from elastic (fast component) and reactive scattering (slow component) are crucial to fit the TOF and LAB data.

However, it is important to address the question whether the emitted hydrogen atom originated from the allyl radical or from the closed-shell hydrocarbon reactants (allene/methylacetylene). Here, we conducted experiments of the allyl radical (41 amu) with D4-methylacetylene and D4-allene (44 amu). If a hydrogen atom elimination prevailed (from the allyl radical), we should have observed signal at $m/z = 84$ ($C_6H_4D_4^+$); however, an atomic deuterium loss pathway (from D4-allene/D4-methylacetylene) should yield $m/z = 83$ ($C_6H_5D_3^+$); note that $m/z = 83$ can in principle originate—if formed—also from dissociative ionization of $C_6H_4D_4$ in the electron impact ionizer of the detector. In the crossed beam experiment at the corresponding center-of-mass angles, we only observed signal at $m/z = 83$ ($C_6H_5D_3^+$). This suggests that only a deuterium atom is emitted from the D4-allene and D4-methylacetyene reactants (eq 4).

$$CD_3CCD + C_3H_5 \rightarrow C_6H_5D_3 + D \quad (4a)$$

$$D_2CCCD_2 + C_3H_5 \rightarrow C_6H_5D_3 + D \quad (4b)$$

Reactions Dynamics of $C_3H_5(X^2A_1)$ with C_3H_4 Isomers

*J. Phys. Chem. A, Vol. 111, No. 23, 2007* **4917**

Therefore, we may conclude that in the crossed beam reactions of the allyl radical with allene and methylacetylene, the hydrogen atom originates from the allene and methylacetylene reactants, too, but not from the allyl radical. Finally, we wanted to narrow down the position of the hydrogen loss in the methylacetylene molecule, i.e., an ejection from the methyl group and/or from the acetylenic carbon atom. Therefore, we crossed the allyl radical beam with D3-methylacetylene (CD_3-CCH) and D1-methylacetylene (CH_3CCD). Only with CD_3CCH we were able to observe an atomic hydrogen via its signal at $m/z = 83$ ($C_6H_5D_3^+$); no hydrogen atom loss was detected with the CH_3CCD reactant. Therefore, we can conclude that the hydrogen atom is eliminated from the acetylenic carbon atom but not from the methyl group of the methylacetylene molecule (eq 5).

$$CD_3CCH + C_3H_5 \rightarrow C_6H_5D_3 + H \qquad (5)$$

Finally, we would like to mention that we also attempted crossed beam reactions of the allyl radical with acetylene and ethylene. The problem with these systems is that due to the reduced center-of-mass angle, the reactive scattering signal is expected to show up between 130 and 160 μs; this would result in an overlap of signal from elastically scattered C_6H_{10}. We recorded up to 10^7 TOF, but it was not feasible due to the overlap with elastically scattered species to assign the reactive scattering signal unambiguously.
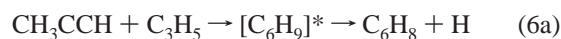
3.2. Center-of-Mass Translational Energy, $P(E_T)$s, and Angular Distributions, $T(\theta)$s. Since the main focus if this paper is the reaction of allyl radicals with allene and methylacetylene, we only discuss the center-of-mass functions of the reactive channels in depth. For both the allene and methylacetylene reactants, the data could be fit with essentially identical translational energy and angular distributions (Figure 3). Best fits of the TOF spectra and of the LAB distributions were acquired with only a single reactive channel fit, i.e., only one center-of-mass translational energy distribution. The $P(E_T)$ extended to a maximum translational energy, E_{max}, of 23−31 kJ mol^{-1}. Recall that the maximum available translational energy is the collision energy minus the reaction energy. Therefore, E_{max} can be utilized to compute the energetics of the title reactions. Here, the reaction to form C_6H_8 isomer(s) under single-collision conditions was found to be endoergic by 98 ± 4 kJ mol^{-1} for both the allene and methylacetylene reactants. Also, in the most favorable case, the most probable translational energy gives information on the order of magnitude of the barrier height in the exit channel, i.e., the atomic hydrogen loss pathway(s).[32] Here, the $P(E_T)$ depicts a maximum of about 10−15 kJ mol^{-1} suggesting the existence of an exit barrier for each reaction. The center-of-mass translational energy distribution also assists us to derive the fraction of total energy available channeling into the translational modes of the products. The averaged fraction of the available energy released into translation was found to be 50 ± 5%. This order of magnitude indicates that the energy randomization in the decomposing complex is likely not complete.[33] It should be highlighted that in order to get an acceptable fit of the data, it was important to include the energy dependence of the reactive cross section via $\sigma(E_C) \sim [1 - E_o/E_C]$. Here, we varied the threshold energies between 50 and 120 kJ mol^{-1}. Best fits were extracted for threshold energies between 105 and 110 kJ mol^{-1}.

In addition to the translational energy distribution, the center-of-mass angular flux distribution, $T(\theta)$, of the atomic hydrogen loss pathway(s) (Figure 3) provides important information on the reaction dynamics. Most importantly, the distribution shows
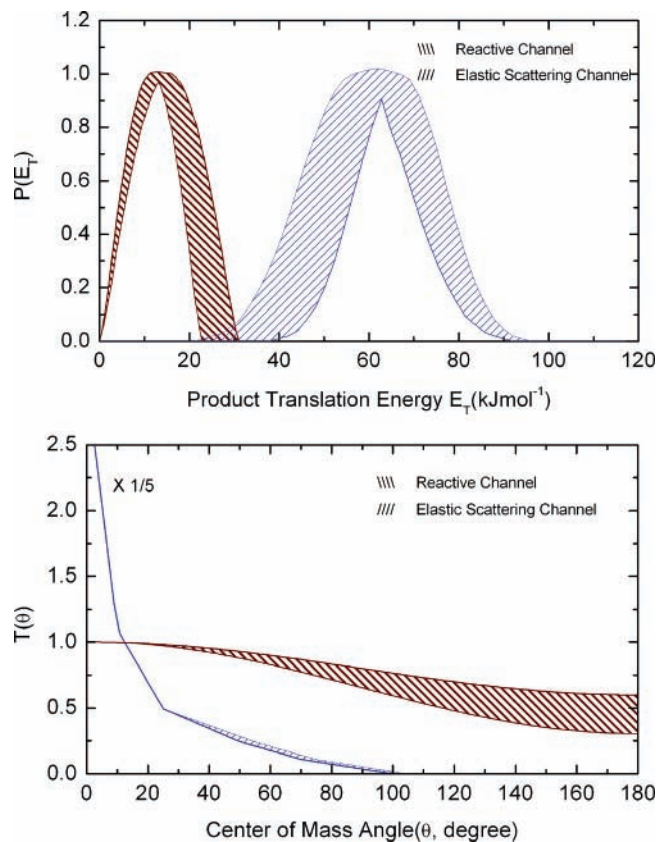
Figure 3. Center-of-mass translational energy (top) and angular flux distributions (bottom) for reactions of allyl with methylacetylene and allene to form C_6H_8 and atomic hydrogen (red). The elastic scatting channel is depicted in blue. For both reactants, data could be fit with essentially identical center-of-mass distributions.

intensity over the complete angular range from 0° to 180°. This finding indicates that the reaction dynamics are indirect and that both reactions of allyl radicals with allene and methylacetylene proceed via formation of C_6H_9 complex(es), $[C_6H_9]^*$, via eq 6.

$$CH_3CCH + C_3H_5 \rightarrow [C_6H_9]^* \rightarrow C_6H_8 + H \qquad (6a)$$

$$H_2CCCH_2 + C_3H_5 \rightarrow [C_6H_9]^* \rightarrow C_6H_8 + H \qquad (6b)$$

Also, the distributions are slightly forward-peaking showing an intensity ratio at the poles of $T(0°)/T(180°) = 1.5 \pm 0.2$. This result suggests the existence of an osculating complex whose lifetime is in the present case similar to the rotational period of the decomposing intermediate(s).[34] Finally, the forward-peaking of the $T(\theta)$ requires that the incorporated allyl radical and the leaving hydrogen atom are located on different sides of the rotational axis.[35] The flux contour map (Figure 4) visualizes the forward-scattering of the C_6H_8 reaction product(s).

4. Discussion

4.1. Energetical Constraints. The center-of-mass translational energy distribution indicates that the reaction to form C_6H_8 plus atomic hydrogen is endoergic by 98 ± 4 kJ mol^{-1}. This reaction energy correlates—within the error limits—with the computed values to synthesize the C_6H_8 isomers 1-hexen-4-yne (**p1**), 1,3,5-hexatriene (**p2**), and 1-hexen-5-yne (**p3**) (Figure 5). Considering the computed reaction paths, it is clear that in the crossed beam studies of allyl with D4-allene and D4-methylacetylene, we only observe a deuterium atom loss but

4918 *J. Phys. Chem. A, Vol. 111, No. 23, 2007*

Guo et al.
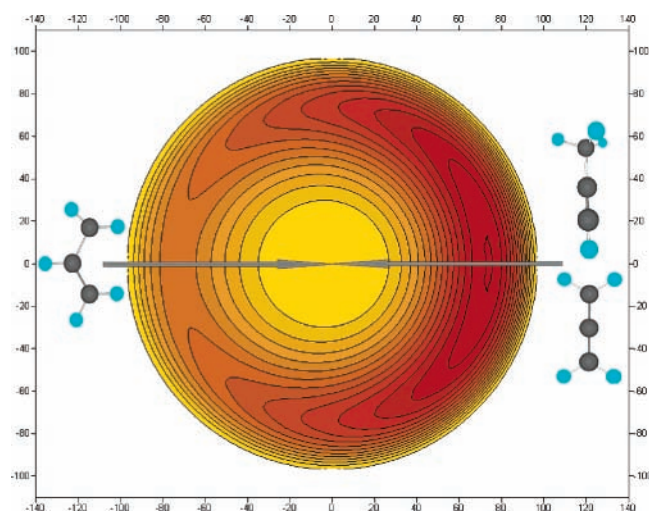
Figure 4. Flux contour map of the C_6H_8 product for the reactions of allyl radicals with methylacetylene and allene; units are given in ms^{-1}.
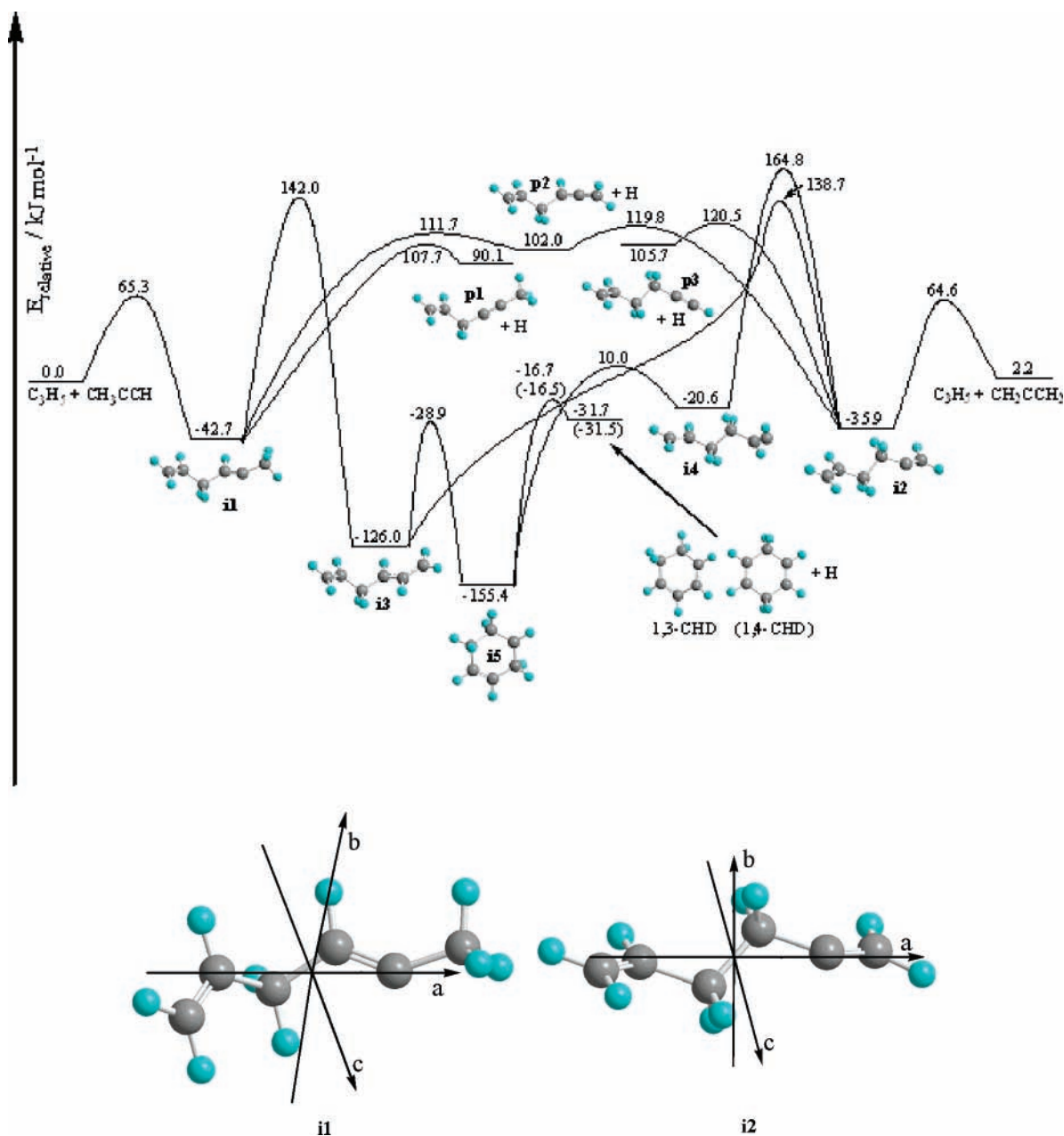
no atomic hydrogen loss from the allyl unit. Here, the allyl unit is conserved during the reaction and formally replaces—in case of D4-allene and D4-methylacetylene—via an exchange reaction a deuterium atom from the closed-shell hydrocarbon reactant. However, since the energetics to form **p1**, **p2**, and **p3** differ by only 15 kJ mol^{-1}, it is difficult to extract from the energetics alone which isomer is formed. We would like to stress that the formation of the 1,3-hexadiene and 1,4-hexadiene isomers cannot be accounted for. First, the computed reaction energy of about −31 kJ mol^{-1} does not correlate with our experimental findings of an endoergic reaction by 98 ± 4 kJ mol^{-1}. Second, 1,3-hexadiene and 1,4-hexadiene can be only formed via a cyclic intermediate **i5**, which is actually accessed from **i3** via **i1** or from **i4** via **i2**. But the transition states of the involved hydrogen shifts are located 142.0 and 164.8 kJ mol^{-1} above the energy of the separated reactants. Considering our collision energies of 124.9 and 124.6 kJ mol^{-1}, it is obvious that these transition states cannot be passed. Third, in case of D4-allene and D4-methylacetylene, the cyclic intermediate **i5** should also show an atomic hydrogen elimination. This has clearly not been observed experimentally. Therefore, based on the reaction energies, energies of the transition states in comparison to the collision energies, and the experimentally failed detection of a hydrogen atom loss pathway, we have to conclude that neither 1,3-hexadiene nor 1,4-hexadiene is formed in our experiment.

4.2. Proposed Reaction Pathways. To unravel which isomer among the energetically accessible **p1**, **p2**, and **p3** structures is formed in the reactions of allyl with methylacetylene and allene, we have first a closer look at the experimental results obtained from the reaction of allyl with (partially) deuterated methylacetylene. Recall that the reaction with CD$_3$CCH only leads to a hydrogen atom loss; no deuterium elimination was observed. Therefore, we propose that the allyl radical attacks the D3-methylacetylene with its terminal carbon atom at the α-carbon atom, i.e., the carbon atom of D3-methylacetylene holding the acetylenic hydrogen atom. This process would lead to an initial addition complex **i1** via indirect scattering dynamics. Recall that the indirect nature of the reaction mechanisms has been inferred from the center-of-mass angular distributions. This addition process is similar, for example, as that found in the reactions of cyano radicals (CN)[36] and D1-ethynyl radicals (CCD)[37] with methylacetylene. Here, the steric hindrance of the bulky methyl group (or D3 methyl group) results in a reduced cone of acceptance of the β-carbon atom of the methylacetylene molecule and hence a preferred addition to the α-carbon atom.

Also, the electron density of the α-carbon atom is larger compared to that of the β-carbon atom. Since the allyl radical is classified as "electron deficient", the regio selective addition is directed to the carbon atom with the higher electron density. Therefore, both the steric hindrance of the methyl group and the enhanced electron density direct the attack of the ally radical to the α-carbon atom forming intermediate **i1**. What is the fate of the latter? As demonstrated earlier, the heights of the transition state of the hydrogen shift eliminates the formation of **i3**. Consequently, this complex must decompose either to **p1** or **p2**. The formation of **p1** correlates with an atomic hydrogen loss; the synthesis of **p2** results solely in the ejection of a deuterium atom from the D3-methyl group. Since we only observed a hydrogen atom emission, in the reaction with D3-methylacetylene, we have to conclude that **p1** is the reaction product in the crossed beam reaction of allyl with methylacetylene/D3-methylacetylene.

How can this be explained? First, since our collision energy is only 13 and 17 kJ mol^{-1} higher than the transition states connecting **i1** to **p2** and **p1**, respectively, we may expect that this slight difference in the energies of the transition states might have a significant effect on the branching ratios of **p1** versus **p2**. Alternatively—due to the large collision energy—we might expect that the lifetime of the intermediate **i1** is too short for a complete energy randomization to occur. This would result in a preferential cleavage of the C−H bond, i.e., the bond in close proximity to the newly formed carbon−carbon bond. In this case, the lifetime of the intermediate would be too short so that the energy can redistribute and "flow" to the acetylenic group leading to a C−D bond rupture. This case has been observed under single-collision conditions in the related reaction of phenyl radicals with D3-methylacetylene leading solely to the formation of C_6H_5−C≡C−CD$_3$.[38] Finally, we would like to point out that the available energy is very close to the reaction threshold. In such situations, small changes in zero-point energies of up to 8 kJ mol^{-1} as found here can influence the outcome of the reaction dramatically when replacing hydrogen by deuterium. If the reaction is statistical, we find branching ratios to form **p1** versus **p2** of 3 (CH$_3$CCH reactant), 12 (CD$_3$CCH reactant), and 166 (CD$_3$CCD). If the reaction is nonstatistical, the formation of **p1** would be even more favorable. Summarized, all the results indicate that in the reaction of the allyl radical with methylacetylene and their (partially) deuterated reactants, the isomer **p1** is formed.

Considering the allyl−allene and allyl−D4-allene reaction, the D4-allene experiment clearly indicates that only a deuterium loss is observed. Therefore, we also propose an initial addition of the allyl radical with its terminal carbon atom to the terminal carbon atom of the allene molecule leading to a doublet intermediate **i2**. Here, a deuterium atom loss can lead to **p2** and/or **p3**. In case of allene, the exit barriers are virtually isoenergetic, and the reaction energies differ by only about 4 kJ mol^{-1}. Again, the energetics alone cannot help to pin down to what extent the atomic hydrogen loss in the allyl−allene system leads to **p2** and/or **p3**. If the reaction is nonstatistical, and hence the lifetime of the reaction intermediated does not allow a complete energy randomization to occur, then we expect a preferential formation of **p2**. Here, the shallow potential energy wells of **i1** and **i2** of only 42.7 and 35.9 kJ mol^{-1} could lead to a relatively short lifetime of the intermediates. In addition, the center-of-mass translational energy distributions assisted to derive the fraction of total energy available channeling into the translational modes of the products to be about 50%; this order of magnitude indicated that that the reaction is fast—too fast

Reactions Dynamics of C$_3$H$_5$(X^{2}A$_1$) with C$_3$H$_4$ Isomers

J. Phys. Chem. A, Vol. 111, No. 23, 2007 **4919**

Figure 5. Upper: stationary points on the doublet C$_6$H$_9$ potential energy surface accessed in the reactions of allyl radicals with methylacetylene and allene. Lower: principal axes of the intermediates **i1** and **i2**.

for a complete energy randomization to occur.[33] Based on these considerations we would expect a preferential formation of **p2**.

4.3. Exit Transition States and Reaction Thresholds. We would like to comment on the existence of the exit transitions states. In both the allyl–allene and ally–methylacetylene reaction, the experimental data suggest the existence of an exit barrier and hence a tight exit transition state in the order of 10–15 kJ mol^{-1}. Considering the closed-shell nature of the reaction products **p1** and **p2/p3**, the reverse reaction of a hydrogen atom addition to a carbon–carbon double and/or triple bond is expected to involve an entrance barrier. As seen in related potential energy surfaces, the addition of a hydrogen atom to an acetylenic and olefinic bond is always correlated with a barrier and therefore a tight exit transition state. The calculations suggest entrance barriers of the reverse hydrogen atom additions of 15–18 kJ mol^{-1}. Therefore, the experimental findings of an exit barrier correlate nicely with the calculated potential energy surface (Figure 5). Most important, in the allyl–methylacetylene and allyl–allene reactions, the leaving hydro-

gen atom and the incorporated allyl unit are on different sides of the *b/c* rotational axis (Figure 5); this was a requirement to account for the forward-peaked center-of-mass angular distributions. The a-like rotations can be likely ruled out.

Finally, it is important to discuss briefly the experimentally found reaction threshold of between 105 and 110 kJ mol^{-1}. Since the reactions were found to be endoergic by 98 ± 4 kJ mol^{-1}, this reaction threshold could indicate either an entrance or an exit barrier. However, an addition of a hydrocarbon doublet radical to carbon–carbon double and triple bonds has typical entrance barriers in the order of up to 50 kJ mol^{-1}—far less than the derived threshold of between 105 and 110 kJ mol^{-1}. On the other hand, the observed endoergicity plus the inferred tight exit transition state located about 15–20 kJ mol^{-1} above the separated products would yield exit transition states located 111 ± 7 kJ mol^{-1} above the separated reactants. These data correlate nicely with the experimentally derived reaction threshold and also with the electronic structure calculations predicting the exit transition states to be located about 108–

121 kJ mol^{-1} above the separated reactants. Therefore, we can conclude that the experimentally derived threshold energy is based on an exit barrier upon decomposition of **i1/i2** to **p1/p2**.

5. Conclusions

We investigated the chemical dynamics of the reaction of allyl radicals, $C_3H_5(X^2A_2)$, with two C_3H_4 isomers, methylacetylene $(CH_3CCH(X^1A_1))$ and allene $(H_2CCCH_2(X^1A_1))$ together with their (partially) deuterated counterparts, under single-collision conditions at collision energies of about 125 kJ mol^{-1} utilizing a crossed molecular beam setup. Our experiments indicate that the reactions are indirect via complex formation and proceed via an addition of the allyl radical with its terminal carbon atom to the terminal carbon atom of the allene and of methylacetylene (α-carbon atom) to form $H_2CCHCH_2CH_2CCH_2$ (**i2**) and $H_2CCHCH_2CHCCH_3$ (**i1**) intermediates, respectively. The lifetimes of these intermediates are similar to their rotational periods but too short for a complete energy randomization to occur. Experiments with D4-allene and D4-methylacetylene indicate that the allyl group stays intact, i.e., no hydrogen emission was observed but only the release of deuterium atoms from D4-allene and D4-methylacetylene. Isotopic substitution experiments combined with the nonstatistical nature of the reaction suggest that **i1** and **i2** decompose preferentially via hydrogen atom elimination to 1-hexen-4-yne (**p1**) and 1,3,5-hexatriene (**p2**), respectively, via tight exit transition states; On the basis of the experiments, the overall reactions to yield **p1** and **p2** from the separated reactants are endoergic by 98 ± 4 kJ mol^{-1}. Our experimental data also correlate with the electronic structure calculations confirming the presence of reaction threshold energies between 105 and 110 kJ mol^{-1}. The observed endoergicities together with the tight exit transition states located about 15−20 kJ mol^{-1} above the separated products yield exit transition states located 111 ± 7 kJ mol^{-1} above the separated reactants. Consequently, the energies of the exit transition states are in line with the experimentally derived threshold energies. On the basis of these energetics, the title reactions are certainly closed at low-temperature, hydrocarbon-rich environments such as in the atmosphere of Saturn's moon Titan and in cold molecular clouds where averaged translational temperatures of about 10 K can be found. However, in high-temperature combustion flames, the reactions of allyl radicals plus methylacetylene and allene can certainly lead to the formation of two C_6H_8 isomers, 1-hexen-4-yne (**p1**) and 1,3,5-hexatriene (**p2**). A possible scenario which is yet to be investigated theoretically or experimentally is that 1,3,5-hexatriene may undergo a unimolecular carbon−hydrogen bond rupture at the C1 atom followed by cyclization, a [6,5]-hydrogen shift, and a final hydrogen atom elimination from the C3 atom yielding ultimately benzene in combustion flames.

References and Notes

(1) (a) Fischer, I.; Chen, P. *J. Phys. Chem. A* **2002**, *106*, 4291. (b) Szpunar, D. E.; Liu, Y.; McCullagh, M. J.; Butler, L. J.; Shu, J. *J. Chem. Phys.* **2003**, *119*, 5078. (c) Robinson, J. C.; Sveum, N. E.; Neumark, D. M. *Chem. Phys. Lett.* **2004**, *383*, 601. (d) Castiglioni, L.; Bach, A.; Chen, P. *J. Phys. Chem.* **2005**, *109*, 962. (e) Castiglioni, L.; Bach, A.; Chen, P. *Phys.*

Chem. Chem. Phys. **2006**, *8*, 2591. (f) Lau, K.-C.; Ng, C. Y. *J. Chem. Phys.* **2005**, *122*, 224310−1. (g) Fan, H.; Pratt, S. T. *J. Chem. Phys.* **2006**, *125*, 144302−1.

(2) (a) Ergut, A.; Levendis, Y. A.; Richter, H.; Carlson, J. Presented at the Fourth Joint Meeting of the U.S. Sections of the Combustion Institute: Western States, Central States, Eastern States, Philadelphia, 2005. (b) Huang, C.; Wei, L.; Yang, B.; Wang, J.; Li, Y.; Sheng, L.; Zhang, Y.; Qi, F. *Energy Fuels* **2006**, *20*, 1505.

(3) (a) Cataldo, F. *Polyynes: Synthesis, Properties and Applications*; Taylor & Francis: New York, 2006. (b) Schüssler, T.; Deyerl, H.-J.; Dümmler, S.; Fischer, I.; Alcara, C.; Elhanine, M. *J. Chem. Phys.* **2003**, *118*, 9077.

(4) Aubry, O.; Delfau, J.-L.; Met, C.; De Barros, M. I.; Vandenbulcke, L.; Vovelle, C. *J. Phys. IV* **2002**, *12*, 75.

(5) Atkinson, D. B.; Hudgens, J. W. *J. Phys. Chem. A* **1999**, *103*, 4242.

(6) Szpunar, D. E.; Liu, Y.; McCullagh, M. J.; Butler, L. J.; Shu, J. *J. Chem. Phys.* **2003**, *119*, 5078.

(7) Mann, D. J.; Hase, W. L. *J. Am. Chem. Soc.* **2002**, *124*, 3208.

(8) Hahn, D. K.; Klippenstein, S. J.; Miller, J. A. *Faraday Discuss.* **2001**, *119*, 79.

(9) Slagle, I. R.; Gutman, D. *Proc. Combust. Inst.* **1986**, *21*, 875. (b) Bacskay, G. B.; Mackie, J. C. *Phys. Chem. Chem. Phys.* **2001**, *3*, 2467.

(10) Mitchell, P.; Frenklach, M. *Phys. Rev. E* **2003**, *67*, 061407.

(11) Kou, J.; Mori, T.; Kubozono, Y.; Mitsuke, K. *Phys. Chem. Chem. Phys.* **2005**, *7*, 119.

(12) Kitajima, A.; Hatanaka, T.; Takeshi, T.; Masao, M.; Torikai, H.; Miyadera, T. *Combust. Flame* **2005**, *142*, 72.

(13) Tsang, W.; Wing, I. Presented at the Fourth Joint Meeting of the U.S. Sections of the Combustion Institute: Western States, Central States, Eastern States, Philadelphia, 2005.

(14) Combustion Chemistry: Elementary Reactions to Macroscopic Processes. *Faraday Discuss.* **2001**, *119*.

(15) http://kinetics.nist.gov/kinetics/index.jsp

(16) (a) Nohara, D.; Sakai, T. *J. Jpn. Pet. Inst.* **1981**, *24*, 103. (b) Tsang, W. *J. Phys. Chem. Ref. Data* **1991**, *20*, 221.

(17) (a) Joo, S.; Kwon, L.; Lee, H.; Choi, J. *J. Chem. Phys.* **2004**, *120*, 7976. (b) Park, J.; Lee, H.; Kwon, H.; Kim, H.; Choi, Y.; Choi, J. *J. Chem. Phys.* **2002**, *117*, 2017. (c) Kwon, H.; Park, J.; Lee, H.; Kim, H.; Choi, Y.; Choi, J. *J. Chem. Phys.* **2002**, *116*, 2675. (d) Leonori, F.; Balucani, N.; Capozza, G.; Segoloni, E.; Stranges, D.; Casavecchia, P. *PCCP* **2007**, *9*, 1307.

(18) (a) Gu, X.; Guo, Y.; Kawamura, E.; Kaiser, R. I. *J. Vac. Sci. Technol., A* **2006**, *24*, 505. (b) Guo, Y.; Gu, X.; Kaiser R. I. *Int. J. Mass Spectrom.* **2006**, *249−250*, 420.

(19) Stranges, D.; Stemmler, M.; Yang, X.; Chesko, J. D.; Suits, A. G.; Lee, Y. T. *J. Chem. Phys.* **1998**, *109*, 5372.

(20) Kohn, D. W.; Clauberg, H.; Chen, P. *Rev. Sci. Instrum.* **1992**, *63*, 4003.

(21) Gu, X.; Guo, Y.; Kawamura, E.; Kaiser, R. I. *J. Vac. Sci. Technol., A* **2006**, *24*, 505−511.

(22) (a) Weiss, M. S. Ph.D. Thesis, University of California, Berkeley, 1986. (b) Vernon, M. Ph.D. Thesis, University of California, Berkeley, 1981. (c) Kaiser, R. I.; Ochsenfeld, C.; Stranges, D.; Head-Gordon, M.; Lee, Y. T. *Faraday. Discuss.* **1998**, *109*, 183.

(23) Kaiser, R. I.; Mebel, A. M.; Balucani, N.; Lee, Y. T.; Stahl, F.; Schleyer, P. v. R.; Schaefer, H. F. *Faraday Discuss.* **2001**, *119*, 51.

(24) Levine, R. D. *Molecular Reaction Dynamics*; Cambridge University Press: Cambridge, 2005.

(25) Becke, A. D. *J. Chem. Phys.* **1993**, *98*, 5648.

(26) Lee, C.; Yang, W.; Parr, R. G. *Phys. Rev. B* **1988**, *37*, 785.

(27) Curtiss, L. A.; Raghavachari, K.; Redfern, P. C.; Baboul, A. G.; Pople, J. A. *Chem. Phys. Lett.* **1999**, *314*, 101.

(28) Purvis, G. D.; Bartlett, R. J. *J. Chem. Phys.* **1982**, *76*, 1910.

(29) Frisch, M. J.; Trucks, G. W.; Schlegel, H. B.; Scuseria, G. E.; Robb, M. A.; Cheeseman, J. R.; Zakrzewski, V. G.; Montgomery, J. A., Jr.; Stratmann, R. E.; Burant, J. C.; Dapprich; Millam, J. M.; Daniels, A. D.; Kudin, K. N.; Strain, M. C.; Farkas, O.; Tomasi, J.; Barone, V.; Cossi, M.; Cammi, R.; Mennucci, B.; Pomelli, C.; Adamo, C.; Clifford, S.; Ochterski, J.; Petersson, G. A.; Ayala, P. Y.; Cui, Q.; Morokuma, K.; Malick, D. K.; Rabuck, A. D.; Raghavachari, K.; Foresman, J. B.; Cioslowski, J.; Ortiz, J. V.; Stefanov, B. B.; Liu, G.; Liashenko, A.; Piskorz, P.; Komaromi, I.; Gomperts, R.; Martin, R. L.; Fox, D. J.; Keith, T.; Al-Laham, M. A.; Peng, C. Y.; Nanayakkara, A.; Gonzalez, C.; Challacombe, M.; Gill, P. M. W.; Johnson, B. G.; Chen, W.; Wong, M. W.; Andres, J. L.; Head-Gordon, M.; Replogle, E. S.; Pople, J. A. *Gaussian 98*, revision A.7; Gaussian, Inc.: Pittsburgh, PA, 1998.

(30) MOLPRO is a package of ab initio programs written by Werner, H.-J. and Knowles, P. J. with contributions from Almlöf, J.; Amos, R. D.; Deegan, M. J. O.; Elbert, S. T.; Hampel, C.; Meyer, W.; Peterson, K.; Pitzer, R.; Stone, A. J.; Taylor, P. R.; Lindh, R.

(31) (a) Eyring, H.; Lin, S. H.; Lin, S. M. *Basic Chemical Kinetics*; Wiley: New York, 1980. (b) Robinson P. J.; Holbrook, K. A. *Unimolecular Reactions*; Wiley: New York, 1972. (c) Steinfield, J. I.; Francisco, J. S.;

Reactions Dynamics of $C_3H_5(X^2A_1)$ with C_3H_4 Isomers

J. Phys. Chem. A, Vol. 111, No. 23, 2007 **4921**

Hase, W. L. *Chemical Kinetics and Dynamics*; Prentice Hall, Engelwood Cliffs, NJ, 1999.

(32) Kaiser, R. I. *Chem. Rev.* **2002**, *102*, 1309.

(33) Kaiser, R. I.; Mebel, A. M. *Int. Rev. Phys. Chem.* **2002**, *21*, 307.

(34) Miller, W. B.; Safron, S. A.; Herschbach D. R. *Discuss. Faraday Soc.* **1967**, *44*, 108.

(35) Kaiser, R. I.; Ochsenfeld, C.; Head-Gordon, M.; Lee, Y. T.; Suits, A. G. *Science* **1996**, *274*, 1508.

(36) Huang, L. C. L.; Balucani, N.; Lee, Y. T.; Kaiser, R. I.; Osamura, Y. *J. Chem. Phys.* **1999**, *111*, 2857.

(37) Kaiser, R. I.; Chiong, C. C.; Asvany, O.; Lee, Y. T.; Stahl, F.; Schleyer, P. v. R.; Schaefer, H. F., III. *J. Chem. Phys.* **2001**, *114*, 3488.

(38) Kaiser, R. I.; Asvany, O.; Lee, Y. T.; Bettinger, H. F.; Schleyer, P. v. R.; Schaefer, H. F., III. *J. Chem. Phys.* **2000**, *112*, 4994.